Bioorganic & Medicinal Chemistry 16 (2008) 9745–9756

Contents lists available at ScienceDirect

Bioorganic & Medicinal Chemistry

journal homepage: www.elsevier.com/locate/bmc

Chalcogenopyrylium dyes as inhibitors/modulators of P-glycoprotein in multidrug-resistant cells

Geri A. Sawada [a], Thomas J. Raub [a], J. William Higgins [a], Nancy K. Brennan [b], Teiah M. Moore [b], Gregory Tombline [b,c], Michael R. Detty [b,*]

[a] Drug Disposition, Eli Lilly and Company, Indianapolis, IN 46285, USA
[b] Department of Chemistry, University at Buffalo, The State University of New York, Buffalo, NY 14260-3000, USA
[c] Department of Microbiology and Immunology, University of Rochester Medical Center, 601 Elmwood Avenue, P.O. Box 607, Rochester, NY 14642, USA

ARTICLE INFO

Article history:
Received 20 August 2008
Revised 24 September 2008
Accepted 26 September 2008
Available online 30 September 2008

Keywords:
Chalcogenopyrylium dyes
P-glycoprotein
Multidrug resistance
Inhibitors
Transporters

ABSTRACT

A series of chalcogenopyrylium dyes were evaluated as modulators/inhibitors of P-glycoprotein (Pgp). Their ability to inhibit verapamil (**VER**)-dependent ATPase activity (IC_{50} values) in lipid-activated, mouse Cys-less mdr3 Pgp was determined. Their ability to promote calcein-AM (**CAM**) uptake in MDCKII-MDR1 cells and their capacity to be transported by Pgp in monolayers of MDCKII-MDR1 cells were also evaluated. The chalcogenopyrylium dyes promoted **CAM** uptake with values of EC_{50} between 5×10^{-6} and 3.5×10^{-5} M and 7 of the 9 dyes examined in transport studies were substrates for Pgp with efflux ratios ($P_{BA/AB}$) between 14 and 390. Binding of three compounds (**1-S**, **3-S**, and **4-S**) to Pgp was also assessed by fluorescence. These three thiopyrylium dyes showed increased fluorescence upon binding to Pgp, giving apparent binding constants, K_{app}, on the order of 10^{-7} to 10^{-6} M. Compound **8-Te** was particularly intriguing since it appeared to influence Pgp at low micromolar concentrations as evidenced by its influence on **VER**-stimulated ATPase activity (IC_{50} of 1.2×10^{-6} M), **CAM** uptake (EC_{50} of 5.4×10^{-6} M), as well as [^{3}H]-vinblastine transport by Pgp in cells (IC_{50} of 4.3×10^{-6} M) and within inside-out membrane vesicles (IC_{50} of 9.6×10^{-6} M). Yet, Pgp did not influence the distribution of **8-Te** in MDCKII-MDR1 monolayers suggesting that **8-Te** may bind to an allosteric site.

1. Introduction

The effective treatment of cancer is often thwarted by the appearance of multidrug resistance (MDR) in patients.[1–3] There are three major mechanisms of drug resistance in cells including decreased uptake of water-soluble drugs that require transporters to enter cells; cellular changes that affect cell cycles, repair of DNA damage, apoptosis, and drug metabolism; and increased efflux by multidrug efflux pumps of hydrophobic drugs that might easily enter the cell via diffusion through the plasma membrane.[1] Multidrug efflux pumps are perhaps the most important contributor to MDR and are capable of expelling multiple chemically and structurally dissimilar drugs from the cell. The expression of the efflux pumps can be up-regulated by exposure to a single chemotherapeutic agent. The mammalian plasma membrane protein P-glycoprotein (Pgp also known as MDR1 or ABCB1) is the most studied MDR efflux protein. Pgp belongs to a larger protein family known as the ATP Binding Cassette (ABC) proteins, the majority of which are transporters.[1] In humans, 48 members of this family are divided into seven subclasses based upon degree of homology.[2] Other important members of this family responsible for MDR in cancer include the multidrug resistance protein series (including multidrug resistance protein 1, MRP1 or ABCC1), breast cancer resistance protein (BCRP, MXR, or ABCG2), and lung-resistance related protein (LRP).[4]

Complicating the treatment of MDR is the fact that Pgp is normally expressed at many physiological barriers including the blood-brain barrier, the apical membranes of the epithelia, the luminal surfaces of colon and small intestine, and kidney proximal tubules.[5] Numerous MDR reversal agents, such as verapamil (**VER**), cyclosporin A, and PSC833 have been examined to minimize the effects of the various efflux pumps.[1,3,6] However, these compounds have major drawbacks, such as alterations in cell metabolism as well as their toxicity toward normal tissues through interactions with normally expressed Pgp. The therapeutic window for these compounds is also severely restricted because the dose necessary for effective inhibition of Pgp, in many cases, exceeds the minimal toxic concentration in normal tissue.[1,7,8] Furthermore, combinations of the modulator and anti-cancer drugs have resulted in unacceptable toxicity, which in turn has caused dose reductions and less effective treatment.[8] Thus, the search remains open for a Pgp modulator/inhibitor that, when administered in combination with chemotherapeutic agent(s), increases the anti-cancer drug uptake, retention and effectiveness.

* Corresponding author. Tel.: +1 716 645 6800x2200; fax: +1 716 645 6963.
E-mail address: mdetty@buffalo.edu (M.R. Detty).

0968-0896/$ - see front matter © 2008 Elsevier Ltd. All rights reserved.
doi:10.1016/j.bmc.2008.09.065

The rhodamines are an interesting class of molecules with respect to their interactions with Pgp. Many drugs have been assayed for competitive transport with rhodamines in the NCI screen.[9] Tetramethylrosamine has been described as the best transport substrate for Pgp both in viable MDR cells and in reconstituted Pgp.[10] Computational studies have suggested that rhodamines and **VER** display compatible features in a rhodamine pharmacophore model.[11] Furthermore, rhodamine derivatives provide a three-dimensional scaffold that can be incorporated into either three-point or four-point pharmacophore models for Pgp.[12]

We have recently examined a small library of tetramethylrosamine derivatives for their ability to stimulate ATPase activity in lipid-activated Cys-less mouse mdr3 Pgp.[13] Within this library, the substituents at the 9-position were varied systematically as well as the chalcogen atom (O, S, Se) within the tricyclic xanthylium core. What was intriguing within this series is that very slight changes in structure gave up to 1000-fold differences in ability to stimulate ATPase activity. Based on these results, we were able to develop a rhodamine-based photosensitizer for drug-resistant CR1R12 cells that over express Pgp that did not require an added inhibitor or modulator to be effective.[14]

As shown in Chart 1, the tricyclic xanthylium core is a rigid pharmacophore fragment that will lock in the spatial orientation of hydrogen bond acceptors and aromatic ring centroids and projection points. Diversity in structural flexibility can only come from substituents in the 9-position. The 2,4,6-trisubstituted chalcogenopyrylium compounds shown in Chart 1 offer similar structural features to the chalcogenorhodamines, but the aromatic centroids and projection points have rotational flexibility and there are several sites for the introduction of structural diversity.

Earlier studies of the chalcogenopyrylium dyes with implanted brain tumors in rats suggested that the chalcogenopyrylium compounds passed the blood–brain barrier.[15] While one reason might be that the blood–brain barrier was compromised by the implantation, an alternative explanation might be that the chalcogenopyrylium photosensitizers were not exported by Pgp and perhaps functioned to inhibit/modulate Pgp. In order to assess whether the chalcogenopyrylium compounds are a new class of Pgp inhibitors/modulators, we have examined a series of these dyes for their ability to inhibit **VER**-induced ATPase activity in lipid-activated Cys-less mouse mdr3 Pgp, for their ability to promote calcein-AM (**CAM**) uptake into MDCKII-MDR1 cells, and for their ability to be transported by Pgp in monolayers of MDCKII-MDR1 cells. While several structural variations were able to inhibit **VER**-induced ATPase activity and to promote **CAM** uptake into MDCKII-MDR1 cells, one telluropyrylium derivative showed minimal stimulation of ATPase activity in addition to inhibiting **VER**-induced ATPase activity in lipid-bound Pgp, promoting **CAM** uptake into and inhibition of [^{3}H]-vinblastine efflux by MDCKII-MDR1 cells, and inhibition of [^{3}H]-vinblastine uptake into Pgp inside-out membrane vesicles.

2. Results

2.1. Selection and synthesis of chalcogenopyrylium compounds

We selected the 17 chalcogenopyrylium dyes shown in Chart 2 from the library of more than 150 similar structures that we have generated over the years. The examples were chosen to resemble the rhodamines and tetramethylrosamines in that at least two amino- or dialkylaminophenyl substituents were present at the 2-, 4-, or 6-positions (Chart 1).[16] The third position, R", among the 2-, 4-, and 6-substituents shown in Chart 1 was substituted with alkyl, heteroaryl, and aryl substituents. The chalcogen atoms were selected from S, Se, and Te. Dyes **9-S**, **11-S**, and **12-Se** were prepared for this study, as shown in Scheme 1, from chalcogenopyranones **15-S**, **16-S**, or **16-Se**.[16c] Values of log*P* for this series of dyes were in the range 0.0–2.4 suggesting that the dyes were available to both aqueous and hydrophobic environments (Table 1).

2.2. Pgp ATPase activity

The chalcogenopyrylium compounds of this study displayed variable ATPase stimulation of lipid-activated, mouse MDR3 Cys-less Pgp, which is 87% identical to human MDR1 Pgp in sequence.[17] ATP hydrolysis was determined via a spectrophotometric-coupled assay. Stock solutions of **VER** and the chalcogenopyrylium dyes were prepared in DMSO. For several of the chalcogenopyrylium dyes in Chart 2 (**1-S**–**4-S**, **7-S**, **8-S**, and **8-Te**) and for **VER**, a specific activity was measured at a "saturating" concentration of drug, that is, at a concentration where ATPase activity was unchanging (typically 5×10^{-5} to 1×10^{-6} M). Specific activities are compiled in Table 1. Basal activity in the presence of DMSO alone (2% by volume, control samples performed in parallel) was 0.48 nmol/min/μg. Control **VER**-stimulated ATPase activity (2×10^{-4} M) for the protein preparation used in this study was roughly 5.4-fold higher at 2.6 nmol/min/μg. At 1×10^{-4} M **3-S**, the specific ATPase activity conferred by compound **3-S** was 1.38 nmol/min/μg. Dyes **1-S**, **8-S**, and **8-Te** conferred specific activities that appeared nearly equivalent to or below basal levels (0.3–0.48 nmol/min/μg) while dyes **2-S**, **4-S**, and **7-S** conferred intermediate specific activities in the 0.70–0.93 nmol/min/μg range (**VER** > **2-S**, **4-S**, **7-S** > **1-S**, **8-S**, **8-Te**).

2.3. Binding of chalcogenopyrylium dyes to Pgp as measured by enhanced fluorescence

While the lack of stimulation of ATPase activity in certain of the chalcogenopyrylium dyes may indicate that these compounds do not interact with Pgp, lack of stimulation of ATPase activity accompanied by strong binding to Pgp is not unprecedented. We have described a subset of rhodamine derivatives where apparent ATPase activities are nearly equivalent to basal values.[18] Values of K_M, the Michaelis–Menton constant, for drug stimulation of ATPase could not be accurately measured in this set, yet these same rhodamine derivatives promoted ATP occlusion at relatively low concentra-

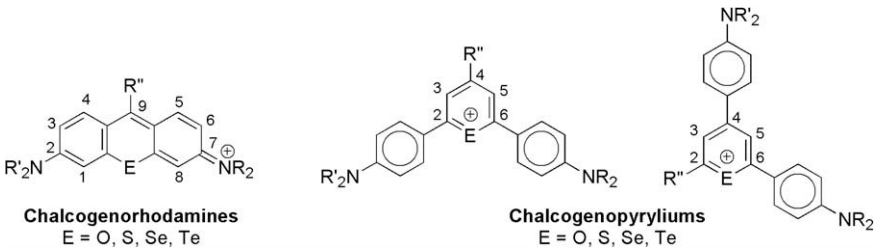

Chart 1.

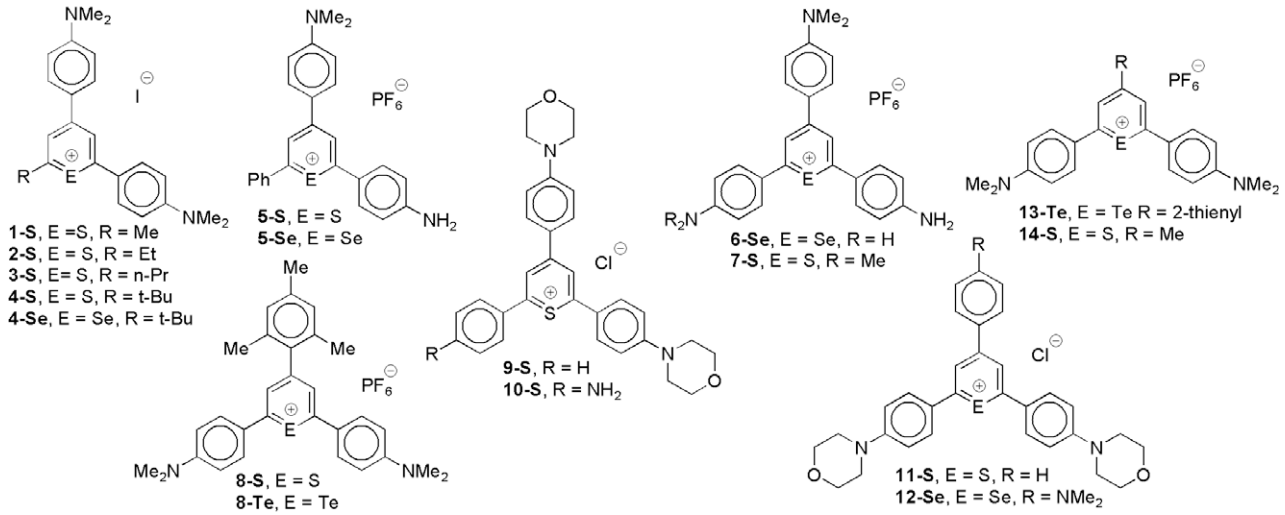

Chart 2. Chalcogenopyrylium dyes of this study.

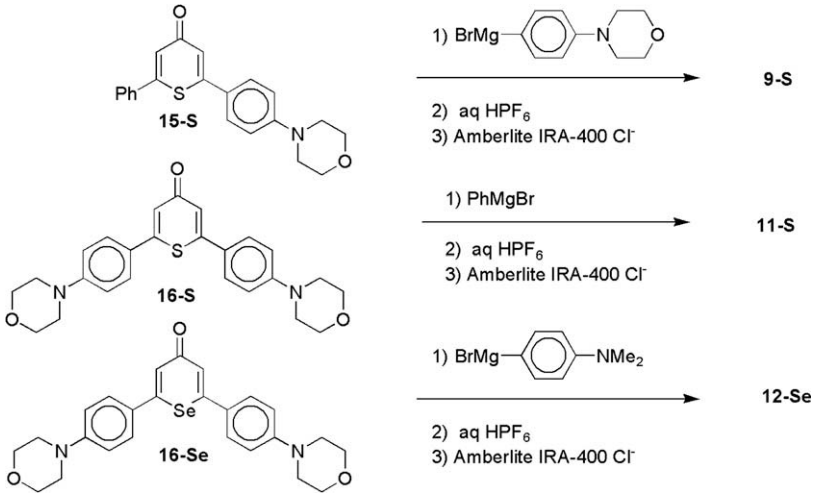

Scheme 1. Preparation of chalcogenopyrylium dyes **9-S**, **11-S**, and **12-Se**.

tions ($\sim 4 \times 10^{-7}$ to 4×10^{-5} M). These data bolster the argument that upon drug binding, the pump partitions to a drug-dependent pathway and basal activity approaches zero.[19] Further, this partitioning phenomenon helps to explain cases where drugs appear to confer ATPase stimulation near or even below basal values, yet they are actually transported by Pgp. In those cases, it is argued that any value above zero is attributed to the weak stimulation by the drug that only appears similar to basal. Moreover, in addition to promotion of ATP occlusion, many rhodamine analogues that failed to confer robust turnover were capable of inhibiting **VER**-dependent ATPase activity at a similar concentration required for ATP occlusion. This provided further evidence for recognition of the analogues by Pgp; however, in these cases a direct measure of binding was not presented.

We have recently shown that the relative fluorescence yields from thiopyrylium dyes **1-S**, **3-S**, and **4-S** increase dramatically (>60-fold) upon binding to DNA relative to solution values.[20] Should the same phenomenon be observed upon binding of these dyes to Pgp, then the enhanced fluorescence would provide a direct indicator of binding to Pgp. Other compounds, including H33342 and LDS-751, show greatly enhanced fluorescence emission upon binding to the drug-binding pocket of Pgp, and this phenomenon has been used to quantify directly drug interaction with purified Pgp.[21]

In order to provide a direct measure of binding to Pgp, we attempted to assay the binding of thiopyrylium dyes **1-S**, **3-S**, and **4-S** using fluorescence. The advantage here compared to the rhodamine series is that, similar to LDS-751, the thiopyrylium dyes display a very weak fluorescence in solution when unassociated with a biopolymer, but display a large increase in quantum yield of fluorescence upon binding.[20] As illustrated in Figure 1 for **4-S**, increasing concentrations of the dyes **1-S**, **3-S**, and **4-S** does not lead to an increase in fluorescence in the absence of Pgp in the presence of 0.2% *Escherichia coli* lipids ("sham" lipids). However, in the presence of 2.5×10^{-7} M Pgp and 0.2% *E. coli* lipids, an increase in fluorescence is observed with increasing concentrations of dye, which can be fit to give values for an apparent binding constant, $K_{app} = 4.7 \pm 0.2 \times 10^{-7}$; $R^2 = 0.99$ for **4-S** (Fig. 1). Similar values were found for **1-S** ($K_{app} = 4.5 \pm 2.9 \times 10^{-6}$ M; $R^2 = 0.95$) and for **3-S** ($K_{app} = 2.2 \pm 1.2 \times 10^{-6}$ M; $R^2 = 0.97$; data not shown). The increase in fluorescence is similar to that observed for binding of dyes **1-S**, **3-S**, and **4-S** to DNA, with emission maxima at 690 nm.[20] These results suggest that the pyrylium dyes can bind to Pgp with micromolar affinities (or lower, e.g., **4-S**) without necessarily conferring robust stimulation of ATPase activity (e.g., the near basal activity found with **1-S**).

Table 1
Values of the *n*-octanol/water partition coefficient (log *P*), IC_{50} for the inhibition of **VER**-induced (2×10^{-4} M) and residual ATPase activity in MDR3 cys-less Pgp, specific activity at a "saturating" dye concentration, EC_{50} for the uptake of **CAM** in MDCKII-MDR1 cells, and % inhibition relative to fully-inhibited MDCKII-MDR1 cells at 5×10^{-6} and 2.5×10^{-5} M chalcogenopyrylium dye

Compound	Log*P*	IC_{50}, $\times 10^{-6}$ M	Residual ATPase activity (nmol/min/μg)	Specific activity (nmol/min/μg)	**CAM** uptake EC_{50}, $\times 10^{-6}$ M	5 μM, % LSN335984	25 μM, % LSN335984
None	—	—	0.4 ± 0.1	0.48 ± 0.10	—	—	—
VER	5.1	—	2.6 ± 0.1	2.60 ± 0.10	5.1 ± 1.2	35 ± 0.65	63 ± 8
1-S	0.6	15	0.5 ± 0.1	0.48 ± 0.10	16 ± 1	13 ± 2	74 ± 2
2-S	0.1	1.0	1.3 ± 0.1	0.74 ± 0.10	—	—	—
3-S	1.2	>100	2.5 ± 0.1	1.37 ± 0.10	9.8 ± 1.1	15.0 ± 0.1	87 ± 2
4-S	1.5	0.88	1.4 ± 0.1	0.70 ± 0.10	7.1 ± 1.1	25 ± 1	60 ± 1
4-Se	1.6	—	—	—	6.7 ± 1.3	23 ± 2	67 ± 1
5-S	0.0	5.3	0.9 ± 0.1	—	14 ± 1	7 ± 1	14 ± 2
5-Se	0.8	—	—	—	20 ± 1	5.0 ± 0.1	22 ± 3
6-Se	2.2	>100	2.5 ± 0.1	—	25 ± 1	6.0 ± 0.2	29 ± 2
7-S	2.2	0.7	1.6 ± 0.1	0.93 ± 0.10	35 ± 1	2.0 ± 0.3	16 ± 1
8-S	2.1	71	0.0 ± 0.1	0.30 ± 0.10	—	—	—
8-Te	2.4	1.2	0.4 ± 0.1	0.44 ± 0.10	5.4 ± 1.0	32 ± 3	230 ± 3
9-S	2.1	30	1.0 ± 0.1	—	—	—	—
10-S	2.1	11	0.7 ± 0.1	—	—	—	—
11-S	1.3	3.1	1.0 ± 0.1	—	—	—	—
12-Se	2.3	55	0.4 ± 0.1	—	—	—	—
13-Te	2.2	7.9	0.9 ± 0.1	—	—	—	—
14-S	1.2	5.7	0.9 ± 0.1	—	—	—	—

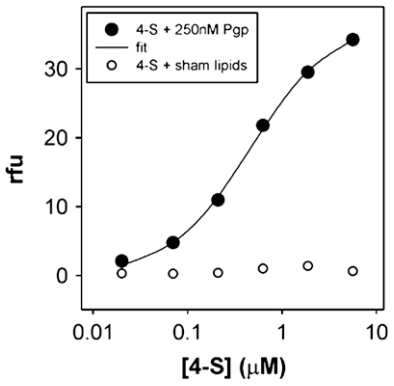

Figure 1. Relative fluorescence of **4-S** in ET buffer and 0.2% *E. coli* lipids with (filled circles) and without (open circles) 2.5×10^{-7} M Pgp. In the presence of Pgp, K_{app} is $(4.7 \pm 0.2) \times 10^{-7}$ M with $R^2 = 0.99$.

2.4. Inhibition of VER-induced stimulation of ATPase activity

The fluorescence studies suggested that the chalcogenopyrylium dyes might be able to inhibit **VER**-induced stimulation of Pgp ATPase activity. We next examined the effect of increasing concentrations of the chalcogenopyrylium dyes on Pgp ATPase activity stimulated by the presence of a fixed, saturating concentration of **VER** (2×10^{-4} M) using lipid-activated, mouse MDR3 Cys-less Pgp. Values of IC_{50}, the concentration giving 50% reduction of the **VER**-induced ATPase stimulation, and the residual ATPase activity (nmol/min/μg), are given in Table 1. Typical plots are shown in Figure 2 for **4-S** and **8-Te**.

This assay indicated that several of the chalcogenopyrylium dyes, in fact, had values of IC_{50} near 10^{-6} M—**2-S**, **4-S**, **5-S**, **7-S**, **8-Te**, **11-S, 13-Te**, and **14-S** (Fig. 2 for **4-S** and **8-Te**). Of the 17 dyes examined, only two (**3-S** and **6-Se**) failed to display an apparent inhibitory effect with values of $IC_{50} > 10^{-4}$ M (Table 1). The majority of the dyes examined had intermediate residual values of ATPase activity as illustrated in Figure 2A for **4-S** with residual ATPase activity of 1.4 nmol/min/μg. Near basal levels of ATPase activity were also observed for the residual ATPase activity with **1-S**, **8-Te** (Fig. 2B), and **12-Se** indicating that in the case of these derivatives, when the chalcogenopyrylium dye reaches its "saturation point," (i.e., higher concentrations would not lower residual ATPase activity further) only very low levels of ATPase activity can be measured.

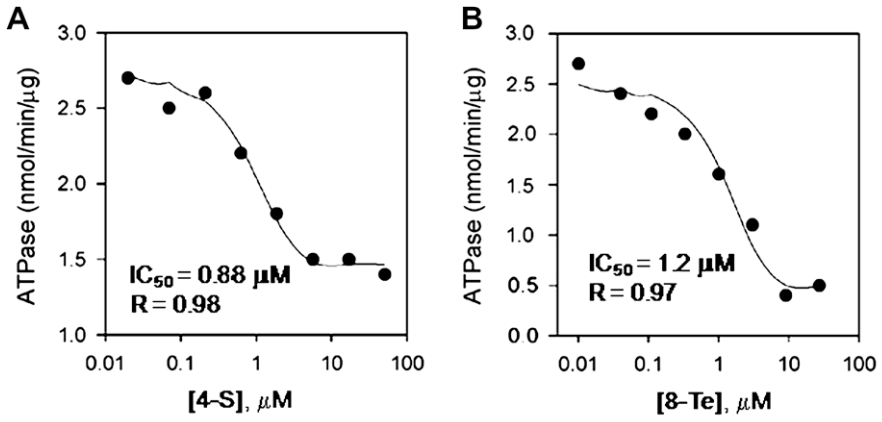

Figure 2. Inhibition of **VER**-induced (2×10^{-4} M) stimulation of ATPase activity in lipid-activated mouse cys-less Pgp with A) thiopyrylium dye **4-S** and B) telluropyrylium dye **8-Te**. Values of IC_{50} were determined by fitting the data to a decreasing slope with a single exponential parameter for the dose-response. Data points were the average of three experiments which showed excellent agreement (<10% standard deviation at each point).

The residual ATPase activity remaining after inhibition of **VER**-induced stimulation of ATPase activity may be due to either residual **VER** stimulation of ATPase or may be due to stimulation by the chalcogenopyrylium dye. If purely competitive inhibition is occurring, the residual ATPase activity should correspond to the residual activity associated with the dye itself. While the residual ATPase activity corresponds nicely to specific activity values for chalcogenopyrylium dyes alone (**1-S, 4-S**, **7-S**, **8-S**, and **8-Te** in Table 1), the possibility of non-competitive inhibition or more complex interactions cannot be ruled out.

In order to address competitive and non-competitive binding of **VER** and the chalcogenopyrylium dyes, we next examined the binding of **VER** and telluropyrylium dye **8-Te** using classical competitive analysis for ATPase inhibition. Competitive analysis has been used by other labs to establish relationships between drugs and Pgp as well as in our analysis of the interaction of rhodamines with **VER**.[18,22] The apparent competitive inhibition pattern of telluropyrylium dye **8-Te** with **VER** is shown in Figure 3. The data were fit to a modified partition equation for competitive inhibition[18,19] where basal ATPase activity is replaced by drug-induced stimulation. In this particular preparation of Pgp, the basal ATPase activity was slightly elevated (0.83 ± 0.03 nmol/min/μg); however, similar to other preparations, maximal **VER**-induced stimulation of ATPase activity, V_{max}, was 2.67 ± 0.08 nmol/min/μg. Importantly, the K_M^D for **VER** stimulation (or the amount of VER required for 50% stimulation), was measured to be $(1.6 \pm 0.4) \times 10^{-5}$ M, which is in excellent agreement with reported K_M^D values of 2×10^{-5} M.[13] Based on these data, non-linear least-squares regression analysis gives a half-maximal inhibition constant, K_i, of $(4 \pm 1) \times 10^{-8}$ M for telluropyrylium dye **8-Te** for inhibition of **VER**-induced stimulation of Pgp ATPase activity.

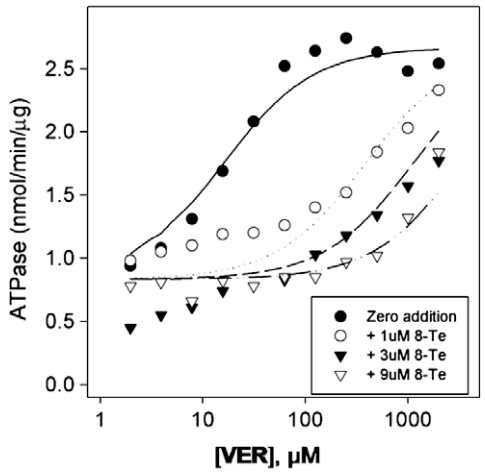

Figure 3. Classic competitive analysis for inhibition of **VER**-dependent ATPase by analogue **5** was conducted as described in Experimental Procedures. The lines represent the non-linear least-squares regression fits of the data to an equation consistent with competitive inhibition which also takes into account the partition model (see reference [18]) and give a K_i of $(4 \pm 1) \times 10^{-8}$ M. Data represent the average of two separate experiments which showed excellent agreement (a standard deviation of <10% for all points).

Although the fits show slight deviation from the raw data at lower **VER** concentrations, the fit appeared more consistent with the data at higher **VER** concentrations. Essentially, while the current data suggest competitive behavior at higher **VER** concentrations, it also appears likely that more complex interactions within the drug binding pocket (or an allosteric site) may exist. Therefore, we hesitate to speculate further until it is possible to perform more detailed experiments that may shed light on stoichiometry and the location of the chalcogenopyrylium binding site(s). Additional knowledge of stoichiometry or further competitive analyses with other drugs may allow additional parameters to be incorporated when fitting the data. It may also be notable that comparison of the apparent competitive behavior of **8-Te** presented herein with the behavior of the rhodamine derivatives analyzed previously also suggests that the interaction of the pyryliums is distinct from the rhodamines, which more closely resembled a strict competitive pattern.

2.5. Enhancement of CAM uptake into MDCKII-MDR1 cells

Selected chalcogenopyrylium compounds were next evaluated for their ability to facilitate the uptake of **CAM** into MDCKII-MDR1 transfected cells, which over express Pgp (or ABCB1).[23] Several of the chalcogenopyrylium compounds with values of IC_{50} near 1×10^{-6} M (**4-S**, **7-S**, and **8-Te**) and two of the chalcogenopyrylium compounds with residual ATPase activity near basal values and values of IC_{50} <2×10^{-5} M (**1-S** and **5-S**) were selected as were compounds **3-S** and **6-Se**, which showed no apparent inhibition of **VER**-induced ATPase activity at concentrations up to 1×10^{-4} M. Uptake of **CAM** was followed by measuring relative fluorescence values obtained after 20-min incubation with **CAM** at 37 °C. These values were plotted as a function of the concentration of dye as shown in Figure 4 for dyes **4-S** and **8-Te**, and values of EC_{50} of uptake of **CAM** are compiled in Table 1.

Interestingly, all nine compounds facilitated the uptake of **CAM** into MDCKII-MDR1 cells including **3-S** (EC_{50} of 9.8×10^{-6} M) and **6-Se** (EC_{50} of 2.5×10^{-5} M). Chalcogenopyrylium dyes **4-S**, **4-Se**,

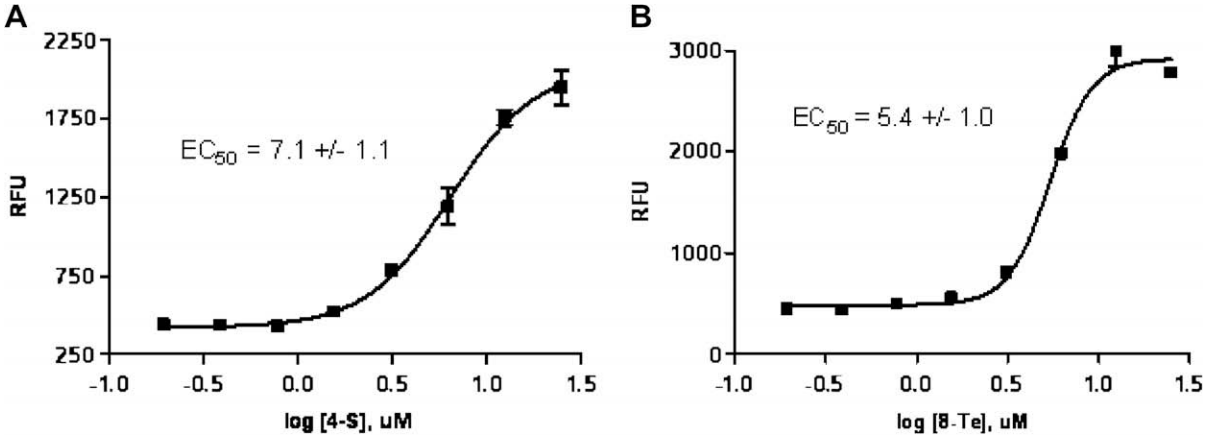

Figure 4. Uptake of **CAM** into MDCKII-MDR1 cells as a function of concentration of (A) chalcogenopyrylium dye **4-S** and (B) chalcogenopyrylium dye **8-Te**. Values of EC_{50} were determined by a sigmoidal dose-response (variable slope) analysis.

and **8-Te** were the three most potent compounds in this assay with values of EC_{50} of 7.1×10^{-6} M, 6.7×10^{-6} M, and 5.4×10^{-6} M, respectively.

As a check of the IC_{50} values, the **CAM** uptake in MDCKII-MDR1 was repeated at concentrations of 5×10^{-6} M and 2.5×10^{-5} M in the chalcogenopyrylium dye and the inhibition of Pgp was compared as a percentage of the inhibition observed with of 2.5×10^{-6} M LSN335984 ($IC_{50} = 4 \times 10^{-7}$ M), which completely inhibits Pgp. LSN335984 is structurally related to the Pgp-specific inhibitor LY335979 or zosuquidar.[3] Values of the percentage inhibition at the two concentrations are given in Table 1. Compounds **1-S**, **3-S**, **4-S**, and **4-Se** were all comparable in this assay with inhibition of 13–25% at 5×10^{-6} M and 60-87% at 2.5×10^{-5} M relative to LSN335984 inhibition. These values are consistent with IC_{50} values between 5×10^{-6} and 2.5×10^{-5} M, which is observed (Table 1). Compound **8-Te** gave 32% inhibition at 5×10^{-6} M and complete inhibition (>100% relative to LSN335984) at 2.5×10^{-5} M, which is consistent with an IC_{50} value near 5×10^{-6} M (observed IC_{50} of 5.4×10^{-6} M, Table 1). In contrast, dyes **6-Se** and **7-S** showed minimal inhibition at 5×10^{-6} M and 2.5×10^{-5} M.

2.6. Transport across monolayers of MDCKII-MDR1 cells

The transport of 5×10^{-6} M solutions of the same set of dyes used to evaluate **CAM** uptake was examined in monolayers of MDCKII-MDR1 transfected cells.[23] MDCKII-MDR1 monolayers display apical and basolateral polarized membranes and are considered to be a near-physiological model for studying Pgp drug transport. In the monolayer, Pgp is asymmetrically distributed being solely present at the apical membrane. In order to evaluate the role of Pgp in the transport of the compounds of this series, transport was measured in the absorptive (apical to basolateral or AB) and secretory (basolateral to apical or BA) transport direction of the cell monolayer, and then calculated an efflux ratio ($P_{BA/AB}$).[24] BSA addition to the buffer was required because a marked fraction of mass added to the donor equilibrated with the cell monolayer for some of the compounds and this resulted in gross underestimation of the permeability constant.[25] The assay was repeated in the presence of 2.5×10^{-6} M LSN335984 to measure transport when Pgp was fully inhibited. The ratio $P_{BA/AB}$ reported in Table 2 is normalized—that is, by dividing $P_{BA/AB}$ in the absence of inhibitor by the secretory/basal ratio observed in the fully inhibited system. Large efflux ratios are assumed to be due to high Pgp-mediated efflux of the compound. Values of passive transport (P_{app}) in the presence of inhibitor, transport in the absorptive (P_{AB}) and secretory (P_{BA}) mode in the absence of inhibitor, the normalized ratio [$P_{BA/AB}$ (no inhibitor)/$P_{BA/AB}$ (with inhibitor)], and the % cell-associated chalcogenopyryliun dye in AB and BA directions in the absence or presence of inhibitor are compiled in Table 2. Of the nine compounds examined in the MDCKII-MDR1 cell monolayer system, seven of the compounds were shown to be Pgp substrates as indicated by net efflux defined by BA/AB P_{app} ratios of 14–390. Curiously, Compounds **7-S** and **8-Te** appeared to be non-substrates as indicated by an efflux ratio of <2. What is most intriguing, especially in the case of **8-Te**, there appeared to be no correlation between the magnitude of the efflux ratio in this assay when compared to inhibition of ATPase or promotion of **CAM** uptake. All nine chalcogenopyrylium dyes showed slow to very slow passive diffusion when Pgp was inhibited by LSN335984 as defined by a decrease in the efflux ratio to ~1.0. It is unclear how the measured 10-fold faster passive P_{app} for compounds **3-S** and **7-S**, albeit still slow or membrane limited, is in response to the *n*-propyl versus *p*-aminophenyl substitutions that were made. Another interesting observation is that P_{AB} for **3-S** in the uninhibited assay is more than an order of magnitude smaller than P_{app} in the fully inhibited system (1.5 nm s^{-1} vs. 22 nm s^{-1}, respectively).

Cell partitioning of the chalcogenopyrylium dyes appears to be highly polarized in the AB direction in the cell monolayers, which suggests that they may reside preferentially in the outer leaflet of the membrane. When Pgp is inhibited with 2.5×10^{-6} M LSN335984, the polarization disappears in seven of the nine compounds and is reduced in the remaining two (**4-S** and **4-Se**, Table 2). In all nine compounds, the % cell-associated dye in the AB direction is reduced in the presence of 2.5×10^{-6} M LSN335984 while the % cell-associated dye in the BA direction is unaffected by 2.5×10^{-6} M LSN335984.

2.7. Inhibition of vinblastine transport in a membrane vesicle model

Compound **8-Te** was evaluated for its ability to inhibit vinblastine transport by Pgp in a membrane vesicle model. The accumulation of [^{3}H]-vinblastine into Pgp membrane vesicles in the presence of **8-Te** (2.5×10^{-7} M to 2.5×10^{-5} M) was monitored, using 5×10^{-6} M LSN335984 as a standard for complete Pgp inhibition. Previously, the inhibition of [3H]-vinblastine accumulation in Pgp membrane vesicles by LSN335984 gave an IC50 value of $(6.5 \pm 1.1) \times 10^{-9}$ M and, thus, complete inhibition of Pgp was assumed at 5×10^{-6} M. Inside-out membrane vesicles[26,27] were prepared from human embryonic kidney ($PEAK^{STABLE}$) cells over expressing human Pgp. Mixtures of [^{3}H]-vinblastine and **8-Te** were added to the vesicles and, following a reaction time of 2.5 min, the vesicles were removed by filtration and the residual radiation on the filter was measured by scintillation counting to give the relative values shown in Figure 5A with an IC_{50} of $(4.3 \pm 1.8) \times 10^{-6}$ M and a slope of 1.8 ± 1.0.

Table 2
Permeability in the MDCKII-MDR1 cell monolayer

Compound	Passive P_{app}[a] nm s^{-1}	P_{AB}, nm s^{-1}	P_{BA}, nm s^{-1}	Efflux ratio[b] $P_{BA/AB}$	Uninhibited % cell[c] (AB/BA)	Inhibited % cell[c,d] (AB/BA)
1-S	4.2 ± 0.7	5.8 ± 0.7	51 ± 11	14	(65 ± 1)/(25 ± 1)	(24 ± 3)/(17 ± 3)
3-S	22 ± 3	1.5 ± 0.7	370 ± 76	390	(27 ± 1)/(11 ± 1)	(8 ± 1)/(11 ± 1)
4-S	3.4 ± 1.1	5.3 ± 0.5	340 ± 38	134	(73 ± 2)/(37 ± 1)	(44 ± 1)/(25 ± 8)
4-Se	2.8 ± 0.7	2.3 ± 0.2	290 ± 6	161	(63 ± 4)/(26 ± 3)	(37 ± 4)/(23 ± 4)
5-S	3.1 ± 0.6	3.7 ± 0.2	170 ± 1	70	(55 ± 1)/(24 ± 1)	(19 ± 1)/(20 ± 1)
5-Se	2.8 ± 0.5	3.5 ± 0.1	120 ± 3	57	(50 ± 1)/(18 ± 1)	(18 ± 1)/(13 ± 4)
6-Se	2.8 ± 0.7	3.4 ± 0.1	45 ± 2	17	(27 ± 1)/(12 ± 1)	(14 ± 1)/(10 ± 1)
7-S	32 ± 0.7	53 ± 4	42 ± 29	1.6	(55 ± 1)/(19 ± 1)	(16 ± 1)/(17 ± 1)
8-Te	4.8 ± 0.7	8.5 ± 0.3	4.2 ± 0.2	1.4	(7 ± 1)/(3 ± 1)	(7 ± 1)/(5 ± 1)

[a] Apparent permeability coefficient with Pgp inhibited by 2.5×10^{-6} M LSN335984.
[b] The ratio of P_{app} in the BA direction to P_{app} in the AB direction divided by the ratio of P_{app} in the BA direction to P_{app} in the AB direction in the fully inhibited system.
[c] % Cell associated is the fraction of mass extracted from the cell monolayer by methanol wash after 1-h flux in the AB or BA direction.
[d] Pgp inhibited by 2.5×10^{-6} M LSN335984.

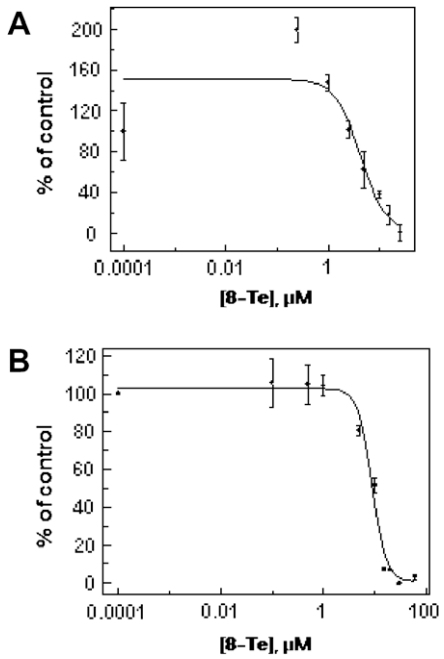

Figure 5. Analyses for inhibition of vinblastine transport by wild-type, human Pgp using **8-Te** were conducted as described in the experimental procedures. (A) Dose response for membrane vesicles from PEAK-MDR1 cells. (B) Dose–response for MDCKII-MDR1 cells. The lines represent the non-linear least-squares regression fits of the data giving IC_{50} values of (4.3 ± 1.8) and (9.6 ± 0.8) × 10^{-6} M, respectively. The slopes of the fits were 1.8 ± 1.0 and 2.5 ± 0.5, respectively. Data represent the average and standard error mean for duplicate measurements. Two separate experiments in different days gave similar results (data are from one of those studies).

2.8. Inhibition of vinblastine efflux by 8-Te in MDCKII-MDR1 cells

[^{3}H]-Vinblastine in an appropriate dilution series with **8-Te** and BSA was introduced to the basolateral chamber of a monolayer of MDCKII-MDR1 transfected cells. The appearance of [^{3}H]-vinblastine in the apical chamber was monitored by scintillation counting as shown in Figure 5B and gave an IC_{50} of (9.6 ± 0.8) × 10^{-6} M with a slope of 2.5 ± 0.5. The vinblastine transport data from both cells and prepared vesicles are also interesting because the inhibition IC_{50} values do correlate with ATPase and CAM inhibition data.

3. Discussion

The goal of this study was to evaluate chalcogenopyrylium dyes as potential Pgp substrates and/or modulators. Given the enhanced flexibility and capacity for chemical variability compared to rhodamines, if tight-binding pyryliums could be uncovered, they could serve as a novel scaffold to develop Pgp inhibitors. Empirically, several structural variations of the chalcogenopyrylium dyes in Chart 2 were able to inhibit **VER**-induced ATPase activity and to promote **CAM** uptake into MDCKII-MDR1 cells. Seven of the nine compounds evaluated in MDCKII-MDR1 cell monolayers were identified as substrates for Pgp with efflux ratios ($P_{BA/AB}$) of 14–390. These dyes appear to be modulators/inhibitors of Pgp function and indeed represent a new class of compounds with this function.

Binding of several of the dyes to Pgp could be demonstrated by the enhanced fluorescence observed with increasing concentration of dye (Fig. 1) suggesting values of K_{app} on the order of 10^{-7} to 10^{-6} M for **1-S**, **3-S**, and **4-S**. While the fluorescence binding studies for these three compounds do not indicate the stoichiometry of binding, one can reasonably infer that most of the Pgp is bound since **VER**-induced stimulation of Pgp is completely inhibited (residual ATPase activity of basal value or less) by several of the dyes (**1-S**, **8-S**, **8-Te**, and **12-Se**).

All nine chalcogenopyrylium dyes that were evaluated with MDCKII-MDR1 cells, including two that showed no apparent inhibition of **VER**-induced ATPase activity (**3-S** and **6-Se**), were effective at promoting **CAM** uptake with EC_{50} values in the 5.4 × 10^{-6} M to 2.5 × 10^{-5} M range. In particular, one telluropyrylium dye, **8-Te** showed a low IC_{50} (1.2 × 10^{-6} M) for inhibiting **VER**-induced ATPase activity, an even lower K_i of 4 × 10^{-8} M for competitive inhibition of **VER**-induced ATPase activity, a low level of residual ATPase activity (0.4 nmol/min/μg) that appears equivalent to basal values, and a low EC_{50} (5.4 × 10^{-6} M) for **CAM** uptake into MDCKII-MDR1 cells.

The lack of inhibition of **VER**-induced ATPase activity with **3-S** was somewhat surprising to us since the fluorescence studies indicated K_{app} of (2.2 ± 1.2) × 10^{-6} M for **3-S** and since **3-S** promotes **CAM** uptake in MDCKII-MDR1 cells with an EC_{50} of 6.4 × 10^{-6} M. Furthermore, at 2.5 × 10^{-5} M **3-S**, 87% of the inhibition of 2.5 × 10^{-6} M LSN335984 (EC_{50} = 4 × 10^{-7} M), which completely inhibits Pgp, was observed with respect to **CAM** uptake (Table 1). The specific activity measured for 1 × 10^{-4} M **3-S** with Pgp was 80% of the specific activity induced by 2 × 10^{-4} M **VER** (Table 1). One possible explanation is that **3-S** binds noncompetitively at an allosteric site with respect to **VER**. A second possibility is that **VER** and **3-S** are exactly compensatory in their interaction with Pgp. Finally, given its low % cell association in the absence of Pgp (see below) differences between experimental conditions or Pgp environment (i.e., membrane composition) may also account for differences in behavior between ATPase and **CAM** experiments.

The possibility that chalcogenopyrylium dyes and **VER** can bind simultaneously to Pgp has ample precedent. Shapiro and Ling[28] described two functional transport sites within Pgp: the R-site, which interacts preferentially with rhodamine 123, and the H-site, which interacts preferentially with H33342. Binding of a drug to one site gives allosteric effects on the other. In their analysis, binding of a drug to the H-site (or R-site) stimulates transport of an R-site (or, conversely, H-site) drug, while inhibiting transport of other H-site (or R-site) drugs. However, it is not clear whether these functional sites have distinct physical locations within the protein. Lugo and Sharom[21b] found that two compounds, rhodamine 123 and LDS-751, which compete with each other for transport by Pgp, can both bind to the R-site simultaneously. In this case, they appeared to interact with each other non-competitively, rather than competitively and the outcome was a 5-fold negative effect on each other's binding. It was suggested that the two drugs may bind to different overlapping regions, or minipockets, within a large flexible binding site.[21b] Loo, Bartlett, and Clarke have shown that a methanethiosulfonate derivative of rhodamine can covalently bind to human Pgp in an activated state.[29] However, ATPase activity of this rhodamine-Pgp complex is further stimulated by **VER** and is inhibited by Hoechst 33342, indicating that covalent attachment of the rhodamine still permits **VER** or Hoechst 33342 to bind to Pgp, presumably at a different site. These same authors have also shown that specific mutations in Pgp affect the binding of specific subsets of drugs again indicating that different binding sites are involved.[30]

In a comparison of thiopyrylium and selenopyrylium dyes, the pairs **4-S**/**4-Se** and **5-S**/**5-Se** showed little difference in **CAM** uptake as a function of heteroatom expressed as values of EC_{50} or as a percentage of LSN335984 in the two-dose inhibition screen (Table 1). In contrast, telluropyrylium dye **8-Te** was far more potent than its thiopyrylium analogue **8-S** at inhibiting **VER**-induced ATPase activity with values of IC_{50} of 1.2 × 10^{-6} M and 7.1 × 10^{-5} M, respectively. Irrespective of IC_{50} values, both **8-S** and **8-Te** had very low values for residual ATPase activity when **VER**-induced ATPase activity was fully inhibited (0.0 and 0.4 nmol/min/μg, respec-

tively). Telluropyrylium dye **13-Te** also displayed a relatively low value of IC_{50} (7.9×10^{-6} M) for **VER**-induced ATPase activity and residual ATPase activity of 0.9 nmol/min/μg.

Mechanistically, the chalcogenopyrylium compounds pose some interesting dilemmas. In isolated Pgp, these compounds have varied effects on **VER**-induced stimulation ranging from no impact at all (**3-S**, **6-Se**) to very low turnover which appears as essentially complete inhibition (**1-S**, **8-S**, **8-Te**, **12-Se**). Of nine compounds examined, seven are substrates for Pgp and two compounds are not (**7-S**, **8-Te**) as determined by the normalized $P_{BA/AB}$ (<2) in MDCKII-MDR1 cells. All nine compounds examined in the transport assay are highly polarized in the % cell-associated assay, but this polarization disappears in the presence of a potent inhibitor of Pgp.

Measurements of the % cell-associated dye (% cell) after 1 h in the permeability assay as a fraction of compound added gave the most intriguing data. The two weakest inhibitors of **VER**-induced ATPase activity, compounds **3-S** and **6-Se**, showed the lowest % cell in the absence of Pgp efflux. This may reflect the local concentration of compound in the cell in the vicinity of the Pgp ATPase stimulating site, which should be reduced more as the transporter is functioning to decrease compound concentration in the cell. However, there is no obvious relationship between % cell and ATPase IC_{50} or **CAM** EC_{50}. One contributing factor could be related to the unusual polarity (>2-fold) in % cell favoring the apical surface when the transporter is patent or uninhibited. In most cases studied for >500 compounds of diverse structure, the % cell lacks polarity (Sawada and Raub, unpublished observation). Upon inhibition of Pgp, this % cell polarity disappeared and was magnitudinally similar to the uninhibited BA % cell value. Exceptions were compounds **4-S** and **4-Se** that had the greatest intrinsic (Pgp inhibited) % cell at >30%.

One possible explanation for this observation is that 2.5×10^{-6} M LSN335984 competes with non-specific binding of the chalcogenopyrylium compounds to the apical membrane. In the presence of inhibitor, the chalcogenopyrylium compounds are free to equilibrate between apical and basal membranes. The polarity observed in the inhibited system with compounds **4-S** and **4-Se** suggests that these two compounds have stronger non-specific binding than other chalcogenopyrylium compounds. However, if this is the case, the structural similarities of **3-S**, **4-S**, and **4-Se** as well as similar values of log*P* (Table 1) suggest that non-specific binding should be similar for all three compounds.

Another explanation is that Pgp maintains a greater concentration of the chalcogenopyrylium compounds in the apical membrane, possibly in the outer leaflet, and upon inhibition of efflux the apical and basal membranes equilibrate. This explanation is consistent with Pgp functioning as either a flippase[31] moving the substrate from the inner to the outer leaflet or as a transporter, where delivery to the apical surface allows diffusion back to the outer membrane.[32] In examples where Pgp is acting as a transporter, high outer membrane association has been noted.[32] Alternatively, interaction with Pgp may occur at an allosteric site that becomes unavailable when an appropriate transport substrate (or other inhibitor) is present. This would be a clear example of a no-competitor effect.

Our examples do not support the idea that other transporters are assisting Pgp in the efflux of the chalcogenopyrylium examples.[33] Overall rates of diffusion in either the AB or BA directions are slow in either the uninhibited or inhibited examples (Table 2), which argue against the active participation of additional transporters. Furthermore, for **8-Te**, values of EC_{50} for the facilitation of **CAM** uptake and IC_{50} for [^{3}H]-vinblastine transport in MDCKII-MDR1 cells (5.4×10^{-6} M and 9.6×10^{-6} M, respectively) are quite similar to values of IC_{50} for inhibition of **VER**-induced stimulation of Pgp in lipid-activated Pgp and IC_{50} for inhibition of [^{3}H]-vinblastine transport in a membrane vesicle model (1.2×10^{-6} M and 4.3×10^{-6} M, respectively). If there are other transporters in the cell membrane in the MDCKII-MDR1 cells, they have minimal impact on the performance of **8-Te** as an inhibitor of Pgp.

Compounds **7-S** and **8-Te** did not appear to be substrates for Pgp based on the normalized $P_{BA/AB}$ of <2. However, **7-S** showed the highest passive P_{app} as well as the highest cell polarity in the uninhibited assay. In contrast, **8-Te** had the lowest values of % cell in either uninhibited or inhibited assays. In the transport assay, neither of these compounds appeared to be recognized by the pump. It is possible that the chalcogenopyrylium compounds show both a no-inhibitor effect[32] as well as competitive inhibition of Pgp. Until Pgp becomes saturated with either substrate or inhibitor, it is possible that neither impacts the function of the other. The range of concentrations may vary markedly among the chalcogenopyrylium compounds where a no-inhibitor effect is observed. As Pgp becomes saturated with either the substrate or inhibitor, competitive recognition then begins. Alternatively, it may be that **8-Te** is a special case among the set, and that this molecule binds at an allosteric site. This reasoning could explain why assays such as ATPase inhibition, **CAM** uptake, and vinblastine transport studies display correlative inhibition values whereas MDCKII-MDR1 studies indicate that Pgp does not influence the cellular distribution of **8-Te.** In this case, competitive inhibition of ATPase relative to **VER** observed in Figure 3 may be the result of a no-competitor effect. That is, **VER** may overcome **8-Te** inhibition at higher concentrations, yet, this may not necessarily reflect overlapping binding sites.

Future studies with these systems can examine flippase versus transporter functions and no-inhibitor versus competitive inhibition behavior over a range of concentrations and with a variety of structural variations. The chalcogenopyrylium dyes offer a more flexible scaffold than the chalcogenorhodamines/rosamines for evaluating structure–activity relationships including selection among the four chalcogen atoms (O, S, Se, and Te) in the chalcogenopyrylium ring as well as the placement of functional groups on alkyl and aryl substituents at the 2-, 4-, and 6-positions. Compounds **1-S, 4-S**, **4-Se**, and **8-Te** represent promising lead structures for further refinement.

Lighter chalcogen analogues of the rhodamines and pyrylium classes, rhodamine 123 and the thiopyrylium compound **AA1** (compound **6-S** with E = S and R = H, Chart 2) have been evaluated as anticancer agents.[34,35] With both the chalcogen-substituted rhodamines and the chalcogenopyrylium compounds, one might be concerned with the toxicity associated with the heavy chalcogen atoms selenium and tellurium. While selenium is an essential trace element and has been the subject of numerous toxicity studies,[36,37] one might be tempted to assume that, since tellurium is below selenium in the periodic table, tellurium must be more metallic and consequently more toxic. Tellurium has been found to be less toxic than selenium based on studies in the semiconductor and reprographic industries, where tellurium is in commercial use.[36,37] Organoselenium compounds, such as Ebselen®, have emerged as viable drug candidates[38] while tellurium-containing compounds have shown acceptable toxicity in animal studies.[39] Ammonium trichloro(dioxoethylene-*O*,*O*')tellurate (AS-101), an inorganic tellurate complex, was shown to have both antitumor and immunomodulatory activity in vivo.[39]

4. Experimental

4.1. General methods

Solvents and reagents were used as received from Sigma–Aldrich Chemical Co. (St. Louis, MO) unless otherwise noted. Concentration in vacuo was performed on a Büchi rotary evaporator. Dry tetrahydrofuran (THF) was obtained by distilling THF from sodium

benzophenone ketyl prior to use. NMR spectra were recorded on an Inova 500 instrument with residual solvent signal as internal standard: $CDCl_3$ (δ 7.26 for proton, δ 77.0 for carbon), CD_2Cl_2 (δ 53.8 for carbon). Infrared spectra were recorded on a Perkin-Elmer FTIR instrument. UV–vis near-IR spectra were recorded on a Perkin-Elmer Lambda 12 spectrophotometer or on a Shimadzu UV-3600 spectrophotometer in quartz cuvettes with a 1-cm path length. Elemental analyses were conducted by Atlantic Microanalytical, Inc. Compounds **1-S, 4-S** and **4-Se** were prepared according to Ref. 16d. Compounds **5-S** and **5-Se** were prepared according to Ref. 16b. Compounds **6-Se**, **7-S**, and **10-S** were prepared according to Ref. 16c. Compounds **8-S**, **8-Te**, **13-Te**, and **14-S** were prepared according to Ref. 16a.

LSN335984 was synthesized by Eli Lilly and Co (Indianapolis, IN). [3H]Vinblastine was obtained from Moravek Biochemicals Inc. (Brea, CA) or GE Healthcare (Buckinghamshire, UK). Puromycin was purchased from Sigma (St. Louis, MO) and $MgCl_2$ from Fisher scientific (Pittsburgh, PA). Most cell culture reagents such as HEPES, Hank's balanced salt solution, Dulbecco's modified Eagle's medium (DMEM), DMEM/F-12, fetal bovine serum and horse serum, gentamicin, phosphate-buffer saline and sucrose buffer were ordered through Invitrogen (Carlsbad, CA). Fetal bovine serum to coat the GF/B filter plates was purchased from Hyclone (Logan, UT). ATP, AMP-PNP, creatine kinase, creatine phosphate and protease inhibitor cocktail tablets were obtained from Roche (Indianapolis, IN).

4.1.1. Preparation of *Δ*-4*H*-2-(4-*N*-morpholinophenyl)-6-phenylthiopyran-4-one (15-S)

Sulfur (0.12 g, 3.8 mmol) and $NaBH_4$ (0.30 g, 7.9 mmol) in 60 mL of 0.25 M NaOEt in EtOH were heated at reflux for several hours until the solution turned clear. 1-(4-*N*-Morpholino-phenyl)-5-phenyl-1,4-pentadiyn-3-one (1.00 g, 3.2 mmol)[16c] was stirred in 0.25 M NaOEt in EtOH (60 mL) at 50 °C until completely dissolved. The resulting solution was then added to the solution of Na_2S at reflux. The reaction mixture was heated at reflux for 2 h and was then concentrated. Water (150 mL) was added and the products were extracted with CH_2Cl_2 (3 × 50 mL). The combined organic extracts were dried over Na_2SO_4 and concentrated. The crude product was purified via chromatography on SiO_2 (20% EtOAc/CH_2Cl_2) and was recrystallized from EtOAc to give 0.43 g (33%) of thiapyranone **15-S**, mp 154–156 °C; ^{1}H NMR [500 MHz, $CDCl_3$] δ 7.60 (m, 7H), 7.08 (s, 2H), 6.93 (AA'BB', 2H, J = 9 Hz), 3.79 (t, 4H, J = 4.8 Hz), 3.20 (t, 4H, J = 4.8 Hz); ^{13}C NMR [126 MHz, $CDCl_3$] δ 182.3, 153.3, 152.9, 152.5, 136.6, 130.8, 129.5, 127.9, 127.2, 127.1, 126.3, 124.9, 115.1, 66.9, 48.3; IR (KBr) 3126, 2962, 1610 cm^{-1}; HRMS (EI) *m/z* 349.1136 (Calcd for $C_{21}H_{19}NO_2S$: 349.1120).

4.1.2. Preparation of 2,4-bis(4-*N*-morpholinophenyl)-6-phenylthiopyrylium chloride (9-S)

A solution of *Δ*-4*H*-2(4-*N*-morpholinophenyl)-6-phenylthiopyran-4-one **15-S** (0.10 g, 0.29 mmol) in THF (5 mL) was added dropwise to a solution of 4-bromo-*N*-phenylmorpholine (0.35 g, 1.4 mmol) and magnesium turnings (0.070 g, 2.8 mmol) in 1 mL of dry THF. The resulting mixture was heated at reflux for 2 h, cooled, and then poured into acetic acid (3 mL). Hexafluorophosphoric acid (60% by weight in water) was added dropwise until a color change was observed. Water (10 mL) was added and the resulting solution was cooled to −10 °C. The resulting precipitate was collected by filtration and the solid was washed with water (10 mL) and ether (10 mL). The crude product was recrystallized from CH_3CN and ether to give 0.16 g (86%) of **9-S (PF_6^-)** as a dark blue solid, mp >260 °C; ^{1}H NMR [500 MHz, CD_2Cl_2] δ 8.52 (s, H), 8.39 (s, 1H), 8.05 (AA'BB', 2H, J = 9 Hz), 7.92 (AA'BB', 4H, J = 9 Hz), 7.85 (m, 2H), 7.69 (m, 3H), 7.08 (m, 4H), 3.86 (t, 8H, J = 4.6 Hz), 3.53 (t, 4H, J = 4.6 Hz), 3.46 (t, 4H, J = 4.6 Hz); λ_{max} (CH_2Cl_2) 606 nm (ε 7.2 × 10^4 M^{-1} cm^{-1}). Anal. Calcd for $C_{31}H_{31}F_6N_2O_2PS$: C, 58.12; H, 4.88; N, 4.37. Found: C, 58.31; H, 4.82; N, 4.52.

The PF_6 salt (0.050 g) was dissolved in 20 mL of CH_3CN and 0.250 g of Amberlite IRA-400 Chloride ion exchange resin was added. The resulting mixture was stirred 0.5 h and was filtered to remove the exchange resin. This process was repeated a total of three times. After the final filtration, the filtrate was concentrated and the residue was recrystallized from CH_3CN/ether to give 0.036 g (88%) of **9-S** as a metallic, purple-gold crystalline solid: mp >260 °C; ^{1}H NMR [500 MHz, CD_2Cl_2] δ 8.52 (s, H), 8.39 (s, 1H), 8.05 (AA'BB', 2H, J = 9 Hz), 7.92 (AA'BB', 4H, J = 9 Hz), 7.85 (m, 2H), 7.69 (m, 3H), 7.08 (m, 4H), 3.86 (t, 8H, J = 4.6 Hz), 3.53 (t, 4H, J = 4.6 Hz), 3.46 (t, 4H, J = 4.6 Hz); λ_{max} (CH_2Cl_2) 606 nm (ε 7.1 × 10^4 M^{-1} cm^{-1}). Anal. Calcd for $C_{31}H_{31}ClN_2O_2S$: C, 62.50; H, 5.16; N, 6.39. Found: C, 62.31; H, 5.14; N, 6.37.

4.1.3. Preparation of *Δ*-4*H*-2,6-bis(4-*N*-morpholinophenyl)-thiopyran-4-one (16-S)

Sulfur (0.10 g, 3.0 mmol) and $NaBH_4$ (0.24 g, 6.2 mmol) in 60 mL of 0.25 M NaOEt in EtOH were heated at reflux for several hours until the solution turned clear. 1,5-Bis(4-*N*-morpholinophenyl)-1,4-pentadiyn-3-one (1.00 g, 2.5 mmol)[16c] was stirred in 0.25 M NaOEt in EtOH (60 mL) at 50 °C until completely dissolved. The resulting solution was then added to the solution of Na_2S at reflux. The reaction mixture was heated at reflux for 2 h and was then concentrated. Water (150 mL) was added and the products were extracted with CH_2Cl_2 (3 × 50 mL). The combined organic extracts were dried over Na_2SO_4 and concentrated. The crude product was recrystallized from EtOAc to give 0.87 g (80%) of thiapyranone **16-S**, mp 218–221 °C; ^{1}H NMR [500 MHz, $CDCl_3$] δ 7.56 (AA'BB', 4H, J = 9 Hz), 7.13 (s, 2H), 6.94 (AA'BB', 4H, J = 9 Hz), 3.86 (t, 8H, J = 4.8 Hz), 3.25 (t, 8H, J = 4.8 Hz); ^{13}C NMR [126 MHz, $CDCl_3$] δ 182.8, 152.7, 152.6, 127.8, 126.5, 124.8, 114.9, 66.6, 48.0; IR (KBr) 2960, 2835, 1509 cm^{-1}; HRMS (EI) *m/z* 434.1678 (Calcd for $C_{25}H_{26}N_2O_3S$: 434.1678).

4.1.4. Preparation of 2,6-bis(4-*N*-morpholinophenyl)-4-phenylthiopyrylium chloride (11-S)

Phenylmagnesium bromide (0.58 mL of a 1.0 M solution, 0.58 mmol) was added dropwise to a solution of thiopyranone **16-S** (0.050 g, 0.12 mmol) in THF (2.5 mL) and the resulting solution was heated at reflux for 2 h. The reaction mixture was cooled and poured into acetic acid (3 mL). Hexafluorophosphoric acid (60% by weight in water) was added dropwise until a color change was observed. Water (10 mL) was added and the resulting solution was cooled to −10 °C. The resulting precipitate was collected by filtration and the solid was washed with water (10 mL) and ether (10 mL). The crude product was recrystallized from CH_3CN and ether to give 0.070 g (91%) of **11-S (PF_6^-)** as a dark blue solid, mp >260 °C; ^{1}H NMR [500 MHz, CD_2Cl_2] δ 8.30 (s, 2H), 7.90 (m, 6H), 7.70 (m, 3H), 7.06 (AA'BB', 4H, J = 9 Hz), 3.86 (t, 8H, J = 4.8 Hz), 3.48 (t, 8H, J = 4.8 Hz); λ_{max} (CH_2Cl_2) 643 nm (ε 6.6 × 10^4 M^{-1} cm^{-1}). Anal. Calcd for $C_{31}H_{31}F_6N_2O_2PS$: C, 58.12; H, 4.88; N, 4.37. Found: C, 58.00; H, 4.83; N, 4.41.

The PF_6 salt (0.050 g) was dissolved in 20 mL of CH_3CN and 0.250 g of Amberlite IRA-400 Chloride ion exchange resin was added. The resulting mixture was stirred 0.5 h and was filtered to remove the exchange resin. This process was repeated a total of three times. After the final filtration, the filtrate was concentrated and the residue was recrystallized from CH_3CN/ether to give 0.038 g (92%) of **11-S** as a metallic, purple-gold crystalline solid: mp >260 °C; ^{1}H NMR [500 MHz, CD_2Cl_2] δ 8.30 (s, 2H), 7.90 (m, 6H), 7.70 (m, 3H), 7.06 (AA'BB', 4H, J = 9 Hz), 3.86 (t, 8H, J = 4.8 Hz), 3.48 (t, 8H, J = 4.8 Hz); λ_{max} (CH_2Cl_2) 643 nm (ε 6.6 × 10^4 M^{-1} cm^{-1}). Anal. Calcd for $C_{31}H_{31}ClN_2O_2S$: C, 70.10; H, 5.88; N, 5.27. Found: C, 70.03; H, 5.81; N, 5.31.

4.1.5. Preparation of 2,6-bis(4-*N*-morpholinophenyl)-4-(4-*N*,*N*-dimethylaminophenyl)-selenopyrylium chloride (12-Se)

A solution of 4*H*-2,6-bis(4-*N*-morpholinophenyl)-selenopyran-4-one **16-Se** (0.10 g, 0.21 mmol)[16c] in THF (5 mL) was added dropwise to a solution of 4-bromo-*N*,*N*-dimethylaniline (0.20 g, 1.0 mmol) and magnesium turnings (0.040 g, 1.7 mmol) in 1 mL of dry THF. The resulting mixture was heated at reflux for 2 h, cooled, and then poured into acetic acid (3 mL). Hexafluorophosphoric acid (60% by weight in water) was added dropwise until a color change was observed. Water (10 mL) was added and the resulting solution was cooled to −10 °C. The resulting precipitate was collected by filtration and the solid was washed with water (10 mL) and ether (10 mL). The crude product was recrystallized from CH_3CN and ether to give 0.15 g (97%) of **12-Se (PF_6^-)** as a blue solid, mp >260 °C; ^{1}H NMR [500 MHz, CD_2Cl_2] δ 8.29 (s, 2H), 8.03 (AA'BB', 2H, J = 9 Hz), 7.81 (AA'BB', 4H, J = 9 Hz), 7.07 (AA'BB', 4H, J = 9 Hz), 6.94 (AA'BB', 2H, J = 9 Hz), 3.89 (t, 8H, J = 4 Hz), 3.44 (t, 8H, J = 4 Hz), 3.22 (s, 6H); λ_{max} (CH_2Cl_2) 636 nm (ε 4.7×10^4 M^{-1} cm^{-1}). Anal. Calcd for $C_{33}H_{36}F_6N_3O_2PSe$: C, 52.95; H, 5.12; N, 5.61. Found: C, 53.25; H, 5.15; N, 5.50.

The PF_6 salt (0.050 g) was dissolved in 20 mL of CH_3CN and 0.250 g of Amberlite IRA-400 Chloride ion exchange resin was added. The resulting mixture was stirred 0.5 h and was filtered to remove the exchange resin. This process was repeated a total of three times. After the final filtration, the filtrate was concentrated and the residue was recrystallized from CH_3CN/ether to give 0.038 g (91%) of **11-S** as a metallic, purple-gold crystalline solid: mp >260 °C; ^{1}H NMR [500 MHz, CD_2Cl_2] δ 8.29 (s, 2H), 8.03 (AA'BB', 2H, J = 9 Hz), 7.81 (AA'BB', 4H, J = 9 Hz), 7.07 (AA'BB', 4H, J = 9 Hz), 6.94 (AA'BB', 2H, J = 9 Hz), 3.89 (t, 8H, J = 4 Hz), 3.44 (t, 8H, J = 4 Hz), 3.22 (s, 6H); λ_{max} (CH_2Cl_2) 636 nm (ε 4.6×10^4 M^{-1} cm^{-1}). Anal. Calcd for $C_{33}H_{36}ClN_3O_2Se$: C, 63.82; H, 5.84; N, 6.77. Found: C, 63.65; H, 6.01; N, 6.78.

4.2. Determination of partition coefficients

The octanol/water partition coefficients were measured using UV–vis spectrophotometry and the 'shake flask' direct measurement.[40] Mixing for 1 h was followed by 4 h of settling time. Equilibration and measurements were made at 23 °C using a Perkin-Elmer Lambda 12 spectrophotometer. HPLC-grade 1-octanol (Sigma–Aldrich) and deionized water were used.

4.3. ATPase assays

ATP hydrolysis determined by the spectrophotometric-coupled assay was performed in microplate format in 96-well plates as previously described.[13] Each reaction contained 4–5 μg of lipid-activated Cys-less mouse mdr3 Pgp with the indicated amount of drug or chalcogenopyrylium compound added in 1-μL volume from concentrated DMSO stock solutions. Cys-less protein was routinely used for ATPase measurements for consistency and to avoid DTT, which is necessary to activate wild-type Pgp, but was found to reduce some of the compounds. DMSO was 2% final in all reactions. Each 50-μL reaction contained 0.040 M Tris–HCl pH 7.4, 1×10^{-4} M EGTA, 0.010 M NaATP, 0.012 M $MgSO_4$, 1×10^{-3} M PEP, 1.5×10^{-3} M NADH, and pyruvate kinase and lactate dehydrogenase (each at a final concentration of 0.1 mg/mL). Reactions were kept on ice and in the dark until placed in the plate reader. Kinetics of NADH oxidation was followed at 37 °C by a decrease in absorption at 340 nm and this was converted into a specific activity for moles ATP hydrolyzed. Control reactions containing DMSO alone or 1.5×10^{-4} M **VER** were performed in parallel for comparison. Assays were performed in a Spectramax Gemini plate reader and analyzed with SOFTmaxPro software. Studies of the inhibition of **VER**-stimulated ATPase (for IC_{50} values) activity were essentially identical except that each reaction contained 2 μg of lipid-activated Pgp and IC_{50} values were determined in the presence of 2×10^{-4} M **VER**.

4.4. Fluorescence assays

Pgp (cys-less) was lipid-activated as described for ATPase studies.[13] Lipids were added at a ratio of 2:1 (w/w) vs. Pgp at a final concentration of 0.2%. Dilutions of the chalcogenopyrylium dyes were added to the microplate (1 μL each) in DMSO (final concentration of DMSO was 2%). Activated Pgp was added to a final concentration of 2.5×10^{-7} M in TE buffer (0.040 M Tris–HCl pH 7.4, 1×10^{-4} M EGTA) to a final volume of 50 μL. Reactions were set up in the dark (minimum indirect light) and the microplate was wrapped in aluminum foil and incubated at 37 °C for 10 min. Control reactions that contained the identical concentration of *E. coli* lipids, but lacking Pgp, were set up in parallel. Fluorescence was measured from the top in a Spectramax M5 Plate Reader at ambient temperature with λ_{EX} = 584 nm and λ_{EM} = 690 nm with a 630-nm cutoff filter. Data (rfu) were plotted using SigmaPlot 2000 software and the fluorescence increase in the presence of Pgp was fit to a hyperbolic curve to determine K_{app}.

4.5. Enhancement of calcein-AM uptake into MDCKII-MDR1 cells

MDCK cells transfected with wild-type MDR1 (ABCB1)[23] were obtained at passage number 12 from Dr. Piet Borst at The Netherlands Cancer Institute. Cell growth was maintained in Dulbecco's Modified Eagle's Medium (Gibco) supplemented with 10% fetal bovine serum (FBS), 100 U/mL penicillin, and 100 μg/mL streptomycin in 75-cm^2 flasks. Cultures were passaged by trypsinization 1:10 twice a week and used at Passage Nos. 16–42. Cells were seeded at 40,000 cells/well in 96-well flat bottom plates (Falcon) using a medium volume of 200 μL, which was replaced on day 3 prior to their use on day 4.

For the two-dose inhibition screen, cells were washed once with Dulbecco's phosphate-buffered saline containing 0.010 M Hepes buffer at pH 7.4 (DPBSH) (Gibco) and incubated in the dark with 80 μL of 5×10^{-6} M or 2.5×10^{-5} M chalcogenopyrylium compound in DPBSH at 37 °C. For the calculation of values of EC_{50}, cells were washed once with DPBSH and incubated with various concentrations of chalcogenopyrylium compound in DPBSH at 37 °C in the dark. Concentrations of the various compounds came from 1:1 serial dilution series with a maximum concentration of 1×10^{-4} M. After 30 min, the test compound was replaced to include 0.5 μg mL^{-1} **CAM** and incubated an additional 20 min in the dark. Calcein fluorescence was read on a Cytofluor series 4000 Multi Well Plate Reader (PerSeptive Biosystems) with λ_{EX} and λ_{EM} set at 485 nm and 530 nm, respectively. Negative (0.25% DMSO in DPBSH), and positive (2.5×10^{-6} M LSN335984, a specific Pgp inhibitor) controls were included in each plate. EC_{50} values were calculated from the serial dilution curves using GraphPad PRISM version 4.03 software. Briefly, compound concentration was plotted as log μM concentration versus relative fluorescence units (rfu) and a sigmoidal dose-response (variable slope) analysis with no weighting or restrictions was applied.

4.6. Pgp-transport studies across MDCKII-MDR1 monolayers

MDCKII-MDR1 cells that were seeded at 5×10^4 cells cm^{-2} onto 12-well (1.13 cm^2 surface area) Transwell polycarbonate filters (Costar) were fed on days 3 and 5, and used on day 6. The upper and lower chamber volumes were 0.5 mL and 1.0 mL, respectively. Cells were rinsed 10 min in DPBSH at 37 °C with mixing on a nuta-

tor (Clay Adams). Cells were pre-incubated with 4.3 mg mL^{-1} bovine serum albumin (BSA) in DPBSH alone or containing 2.5×10^{-6} M LSN335984. After 30 min, 5×10^{-6} M test compound in BSA/DPBSH with or without inhibitor was added to the donor chamber (0.5 mL upper or apical, 1.0 mL lower or basolateral). Initial donor samples were taken at $t = 0$. For apical-to-basolateral (A–B) flux, D_0 was taken from the mixing tube before addition to the cell monolayer. For basolateral-to-apical (B–A) flux this sample was taken from the 12-well plate 10 min after transfer, but before cell wells were added. Samples were taken from both the donor and receiver chambers following a 1-h incubation in the dark at 37 °C with constant mixing by nutation. Cell monolayers were rinsed briefly two times using cold DPBS and extracted with 500 μL methanol for 3 min.

The concentration of analytes was determined by LC-MS/MS after dilution of samples with equal part methanol. Chromatography was effected on a Javelin BETASIL C18 column (20 × 2.1 mm, 5 μ) at a flow rate of 1.5 mL min^{-1} using a gradient of 40% mobile phase B with a hold time of 0.1 min, followed by a 0.1 min linear gradient to 80% B with a hold time of 0.15 min, followed by a step gradient to 98% B with a hold time of 0.4 min where mobile phase A is water/TFA/1 M NH_4HCO_3 (20,000:8:2, v/v) and mobile phase B is ACN/TFA/1 M NH_4HCO_3 (2000:8:2, v/v) Column eluent was diverted to waste from 0 to 0.15 min and then introduced into a Sciex API 4000 triple quadrupole mass spectrometer with turboionspray source operated in the positive mode at 740 °C for 0.3 min. MRM experiments monitored were: 349/333 for **1-S**; *m/z* 377/361 for **3-S**; *m/z* 391/375 for **4-S**; *m/z* 439/423 for **4-Se**; *m/z* 383/367 for **5-S**; *m/z* 431/351 for **5-Se**; *m/z* 446/366 for **6-Se**; *m/z* 427/351 for **7-S**; and *m/z* 551/134 for **8-Te**.

4.7. Inhibition of vinblastine efflux in MDCKII-MDR1 cells by 8-Te

MDCKII-MDR1 cells were seeded onto Costar Transwell polycarbonate membranes and maintained as previously described. On day 6, cells were rinsed 1 × 10 min in DPBSH with nutation at 37 °C, and then conditioned in 0, 0.1, 0.5, 1, 5, 10, 20, or 40 × 10^{-6} M **8-Te** in BSA/DPBSH in the dark. After 30 min at 37 °C, 1.0 mL [^{3}H]-vinblastine (0.25 μCi mL^{-1} from 0.1 mCi mL^{-1} EtOH stock) in appropriate **8-Te** solution was introduced to the basolateral chamber and 0.5 mL fresh **8-Te** was added to the apical chamber. The incubator was maintained in the dark during experiments. Initial donor samples were taken from the basolateral chamber at $t = 0$. The apical solution was replaced every 10 min with fresh buffer and appearance of [^{3}H]-vinblastine in the apical chamber was measured by scintillation counting. An EC_{50} was calculated using XLfit software.

4.8. Inhibition of vinblastine efflux in a membrane vesicle model by 8-Te

Human embryonic kidney ($PEAK^{STABLE}$) cells over expressing human Pgp were obtained from William Perry at Eli Lilly and Company. The detailed transfection procedure for development of this cell line was described by Godinot et al.[41] PEAK-MDR1 cells were grown in 5% CO_2 at 37 °C in a humidified atmosphere in DMEM supplemented with 10% fetal bovine serum, 50 μg/mL gentamicin, and 0.5 μg/mL puromycin. Cells were grown in monolayers until they reached 80% confluency and passaged twice before being adopted to suspension culture. Cells grown in suspension were cultured in spinner flasks containing modified DMEM/F-12 medium supplemented with 2% horse serum and 0.3 μg/mL puromycin until total cell number was approximately 10^9 cells.

4.9. Isolation of membrane vesicles

Plasma membranes were prepared by nitrogen decompression and differential centrifugation as described by Lever[26] with modification. Cultured PEAK-MDR1 cells were centrifuged at 800g for 5 min at 4 °C. Cells were re-suspended in 50 mL phosphate-buffer saline, pH 7.4 at 4 °C, and washed once with 50 mL 2×10^{-4} M $MgCl_2$-sucrose buffer by centrifugation at 800g for 5 min at 4 °C. The cell pellet was washed once with 2×10^{-4} M $CaCl_2$-sucrose buffer supplemented with protease inhibitor cocktail (1 protease inhibitor cocktail tablet per 50 ml $CaCl_2$-sucrose buffer) before equilibration for 30 min at 150 p.s.i. of nitrogen pressure in the cell disruption bomb (Parr Instrument Co., Moline, IL). Cells were burst by slow release of pressure. After removal of nuclei and unbroken cells by centrifugation at 800g for 5 min at 4 °C, the supernatant was supplemented with 0.001 M EDTA. The supernatant was layered onto a 35% sucrose buffer cushion containing 0.01 M Tris, 0.001 M EDTA, and pH 7.4 and centrifuged at 16,000g for 1 h at 4 °C. Membranes collected at the interface were subsequently pelleted at 100,000g for 1 h at 4 °C, re-suspended in 0.25 M sucrose, and passed through a 25-ga. needle to vesicularize the membrane preparation.[27] The prepared membrane vesicles were stored in a liquid nitrogen freezer. The protein concentration of the vesicle preparation was determined using the bicinchoninic acid method described by Smith et al.[42]

The inhibition assay was conducted using 1×10^{-7} M [^{3}H]-vinblastine (0.25 μCi mL^{-1}) as a Pgp substrate. The accumulation of [^{3}H]-vinblastine into Pgp membrane vesicles was inhibited by **8-Te** (2.5×10^{-7} M–2.5×10^{-5} M), using 5×10^{-6} M LSN335984 as a standard for complete Pgp inhibition. Previously, the inhibition of [^{3}H]-vinblastine accumulation in Pgp membrane vesicles by LSN335984 was shown to exhibit an IC_{50} value of $(6.5 \pm 1.1) \times 10^{-9}$ M and thus a complete inhibition of Pgp was assumed at 5×10^{-6} M. The reaction mixtures contained 0.004 M ATP, ATP with different concentrations of **8-Te** (2.5×10^{-7} M–2.5×10^{-5} M), ATP with 5×10^{-6} M LSN335984, or 0.004 M AMP-PNP. All reaction mixtures contained 1×10^{-7} M [^{3}H]-vinblastine, the regenerating system including 100 μg mL^{-1} creatine kinase, 0.010 M creatine phosphate, and 0.010 M $MgCl_2$. The reaction was started by addition of 30 μL reaction mixtures to vesicles (20 μg/20 μL) or 20 μL sucrose buffer. The reactions were incubated for 2.5 min at 37 °C with gentle agitation in the dark. The reactions were stopped by the addition of ice-cold sucrose buffer to wells and filtered onto a membrane filter (GF/B glass fiber plate soaked overnight in 10% FBS/0.25 M sucrose buffer, v/v) with a 96-channel cell harvester (PerkinElmer, Boston, MA). Radioactivity retained on the filter was determined by liquid scintillation counting.

4.10. Calculations for inhibition studies

All values were corrected for background. The background was determined by the accumulation of [^{3}H]-vinblastine in the presence of 5×10^{-6} M LSN335984, which completely inhibits [^{3}H]-vinblastine uptake mediated by Pgp. The calculation of the concentration of inhibitor resulting in 50% inhibition (IC_{50} value) was then determined by nonlinear regression analysis using WinNonlin Professional, version 5.0.1 (Pharsight Corporation, Mountain View, CA), where % activity in relation to control = $100 \times \frac{DPM_{max}}{(1+\frac{[I]}{IC_{50}})^s}$, [I] = inhibitor concentration, DPM_{max} is the highest [^{3}H]-vinblastine uptake with background corrected, and s is the slope factor.

Acknowledgments

This research was supported in part by NIH Grant T32 CA09363 (Postdoctoral Training Grant) to G.T. G.T. gratefully acknowledges

Alan Senior, Robert Bambara, and Barbara Iglewski for encouragement and the use of their laboratory space and supplies. We thank Dr. Piet Borst at The Netherlands Cancer Institute for supplying the MDCKII-MDR1 cells and William Perry at Eli Lilly and Company for the human embryonic kidney (PEAK^{STABLE}) cells.

References and notes

1. (a) Gottesman, M. M.; Fojo, T.; Bates, S. E. *Nature Rev./Cancer* **2002**, *2*, 48; (b) Szakacs, G.; Paterson, J. K.; Ludwig, J. A.; Booth-Genthe, C.; Gottesman, M. M. *Nature Rev./Drug Discov.* **2006**, *5*, 219.
2. Dean, M.; Rzhetsky, A.; Allikmets, R. *Genome Res.* **2001**, *11*, 1156.
3. (a) Seelig, A.; Gatlik-Landwojtowicz, E. *Mini-Rev. Med. Chem.* **2005**, *5*, 135; (b) Raub, T. J. *Mol. Pharm.* **2006**, *3*, 3.
4. Burger, H.; Foekens, J. A.; Look, M. P.; Meijer-van Gelder, M. E.; Klijn, J. G. M.; Wiemer, E. A. C.; Stoter, G.; Nooter, K. *Clin. Cancer Res.* **2003**, *9*, 827.
5. Loscher, W.; Potschka, H. *Nat. Rev. Neurosci.* **2005**, *6*, 591.
6. (a) Tiberghien, F.; Loor, F. *Anti-Cancer Drugs* **1996**, *7*, 568; (b) Hirsch-Ernst, K. I.; Ziemann, C.; Rustenbeck, I.; Kahl, G. F. *Toxicology* **2001**, *167*, 47; (c) Loor, F.; Tiberghien, F.; Wenandy, T.; Didier, A.; Traber, R. *J. Med. Chem.* **2002**, *45*, 4598.
7. Fisher, G. A.; Lum, B. L.; Hausdorff, J.; Sikic, B. I. *Euro. J. Cancer* **1996**, *32A*, 1082.
8. Fojo, T.; Bates, S. *Oncogene* **2003**, *22*, 7512.
9. (a) Lee, J. S.; Paull, K.; Alvarez, M.; Hose, C.; Monks, A.; Grever, M.; Fojo, A. T.; Bates, S. E. *Mol. Pharm.* **1994**, *46*, 627; (b) Scala, S.; Akhmed, N.; Rao, U. S.; Paull, K.; Lan, L.-B.; Dickstein, B.; Lee, J.-S.; Elgemeie, G. H.; Stein, W. D.; Bates, S. E. *Mol. Pharm.* **1997**, *51*, 1024.
10. (a) Eytan, G. D.; Regev, R.; Hurwitz, C. D.; Assaraf, Y. G. *Eur. J. Biochem.* **1997**, , *248*, 104; (b) Lu, P.; Liu, R.; Sharom, F. J. *Eur. J. Biochem.* **2001**, *268*, 1687; (c) Loetchutinat, C.; Saengkhae, C.; Marbeuf-Gueye, C.; Garnier-Suillerot, A. *Eur. J. Biochem.* **2003**, *270*, 476.
11. Pajeva, I. K.; Wiese, M. *J. Med. Chem.* **2002**, *45*, 5671.
12. (a) Raub, T. J. *Mol. Pharm.* **2006**, *3*, 3; (b) Li, W.-X.; Li, L.; Eksterowicz, J.; Ling, X. B.; Cardozo, M. *J. Chem. Inf. Model.* **2007**, *47*, 2429.
13. Tombline, G.; Donnelly, D. J.; Holt, J. J.; You, Y.; Ye, M.; Gannon, M. K.; Nygren, C. L.; Detty, M. R. *Biochemistry* **2006**, *45*, 8034.
14. Holt, J. J.; Gannon, M. K.; Tombline, G.; McCarty, T. A.; Page, P. M.; Bright, F. V.; Detty, M. R. *Biorg. Med. Chem.* **2006**, *14*, 8635.
15. Powers, S. K.; Walstad, D. L.; Brown, J. T.; Detty, M. R.; Watkins, P. J. *J. Neuro-Oncol.* **1989**, *7*, 179–185.
16. (a) Leonard, K. A.; Nelen, M. I.; Simard, T. P.; Davies, S. R.; Gollnick, S. O.; Oseroff, A. R.; Gibson, S. L.; Hilf, R.; Chen, L. B.; Detty, M. R. *J. Med. Chem.* **1999**, *42*, 3953–3964; (b) Leonard, K. A.; Hall, J. P.; Nelen, M. I.; Davies, S. R.; Gollnick, S. O.; Oseroff, A. R.; Gibson, S. L.; Hilf, R.; Chen, L. B.; Detty, M. R. *J. Med. Chem.* **2000**, *43*, 4488–4498; (c) Brennan, N. K.; Hall, J. P.; Davies, S. R.; Gollnick, S. O.; Oseroff, A. R.; Gibson, S. L.; Hilf, R.; Detty, M. R. *J. Med. Chem.* **2002**, *45*, 5123–5135; (d) McKnight, R. E.; Ye, M.; Ohulchanskyy, T. Y.; Sahabi, S.; Wetzel, B. R.; Wagner, S. J.; Skripchenko, A.; Detty, M. R. *Bioorg. Med. Chem.* **2007**, *15*, 4406–4418.
17. Tombline, G. L.; Urbatsch, I. L.; Virk, N.; Muharemagic, A.; Bartholomew White, L.; Senior, A. E. *Arch. Biochem. Biophys.* **2006**, *445*, 124.
18. Tombline, G.; Holt, J. J.; Gannon, M. K.; Donnelly, D. J.; Wetzel, B.; Sawada, G. A.; Raub, T. J.; Detty, M. R. *Biochemistry* **2008**, *47*, 3294.
19. (a) Al-Shawi, M. K.; Polar, M. K.; Omote, H.; Figler, R. A. *J. Biol. Chem.* **2003**, *278*, 52629; (b) Omote, H.; Fiegler, R. A.; Polar, M. K.; Al-Shawi, M. K. *Biochemistry* **2004**, *43*, 3917.
20. Ohulchanskyy, T. Y.; Gannon, M. K., II; Ye, M.; Wagner, S. J.; Skripchenko, A.; Prasad, P. N.; Detty, M. R. *J. Phys. Chem. B* **2007**, *111*, 9686.
21. (a) Qu, Q.; Chu, J. W.; Sharom, F. J. *Biochemistry* **2000**, *42*, 1345–1353; (b) Lugo, M. R.; Sharom, F. J. *Biochemistry* **2005**, *44*, 14020–14029; (c) Lugo, M. R.; Sharom, F. J. *Biochemistry* **2005**, *44*, 643–655.
22. Litman, T.; Zeuthen, T.; Skovsgaard, T.; Stein, W. D. *Biochim. Biophys. Acta* **1997**, *1361*, 169.
23. Evers, R.; Kool, M.; Smith, A. J.; van Deemter, L.; de Haas, M.; Borst, P. *Br. J. Cancer* **2000**, *83*, 366.
24. Troutman, M. D.; Thakker, D. R. *Pharm. Res.* **2003**, *20*, 1192–1199.
25. Sawada, G. A.; Barsuhn, C. L.; Lutzke, B. S.; Houghton, M. E.; Padbury, G. E.; Ho, N. F. H.; Raub, T. J. *J. Pharm. Exp. Therap.* **1999**, *288*, 1317–1326.
26. Lever, J. E. *Biochem. Biophys. Res. Commun.* **1977**, *79*, 1051.
27. Dantzig, . A. H.; Shepard, R. L.; Cao, J.; Law, K. L.; Ehlhardt, W. J.; Baughman, T. M.; Bumol, T. F.; Starling, J. J. *Cancer Res.* **1996**, *56*, 4171.
28. Shapiro, A. B.; Ling, V. *Eur. J. Biochem.* **1997**, *250*, 130–137.
29. Loo, T. W.; Bartlett, M. C.; Clarke, D. M. *J. Biol. Chem.* **2003**, *278*, 50136.
30. Loo, T. W.; Bartlett, M. C.; Clarke, D. M. *J. Biol. Chem.* **2007**, *22*, 32043.
31. (a) Eckford, P. D. W.; Sharom, F. J. *Biochem. J.* **2005**, *389*, 517; (b) Sharom, F. J. *Biochem. Cell Biol.* **2006**, *84*, 979.
32. Acharya, P.; Tran, T. T.; Polli, J. W.; Ayrton, A.; Ellens, H.; Bentz, J. *Biochemistry* **2006**, *45*, 15505.
33. Acharya, P.; O'Connor, M. P.; Polli, J. W.; Ayrton, A.; Ellens, H.; Bentz, J. P. *Drug Metab. Dispos.* **2008**, *36*, 452.
34. Bernal, S. D.; Lampdis, T. J.; McIsaac, R. M.; Chen, L. B. *Science* **1986**, *222*, 169.
35. Sun, X.; Wong, J. R.; Song, K.; Hu, J.; Garlid, K. D.; Chen, L. B. *Cancer Res.* **1994**, *54*, 1465.
36. Fishbein, L. In *Metals and Their Compounds in the Environment*; Merian, E., Ed.; VCH Publishers: New York, 1991; pp 1211–1226. Chapter II.28.
37. Longnecker, M. P.; Taylor, P. R.; Levander, O. A.; Howe, M.; Veillon, C.; McAdam, P. A.; Patterson, K. Y.; Holden, J. M.; Stampfer, M. J.; Morris, J. S. *Am. J. Clin. Nutr.* **1991**, *53*, 1288.
38. Mugesh, G.; DuMont, W.-W.; Sies, H. *Chem. Rev.* **2001**, *101*, 2125.
39. (a) Nyska, A.; Waner, T.; Pirak, M.; Albeck, M.; Sredni, B. *Arch. Toxicol.* **1989**, *63*, 386–393; (b) Sredni, B.; Caspi, R. R.; Klein, A.; Kalechman, Y.; Danziger, Y.; BenYa'akov, M.; Tamari, T.; Shalit, F.; Albeck, M. *Nature* **1987**, *330*, 173–176; c Albeck, M.; Pavliv, L.; Sredni, B. New Complexes of Tellurium and Selenium Compounds Having Improved Solubility, for Induction of Cytokine(s). DK Patent 167148B, 1993.
40. Sangster, J. In *Octanol–Water Partition Co-efficients: Fundamentals and Physical Chemistry*; Fogg, P. G. T., Ed.; John Wiley and Sons: New York, 1997.
41. Godinot, N.; Iversen, P. W.; Tabas, L.; Xia, X.; Williams, D. C.; Dantzig, A. H.; Perry, W. L. *Mol. Cancer Ther.* **2003**, *2*, 307.
42. Smith, P. K.; Krohn, R. I.; Hermanson, G. T.; Mallia, A. K.; Gartner, F. H.; Provenzano, M. D.; Fujimoto, E. K.; Goeke, N. M.; Olson, B. J.; Klenk, D. C. *Anal. Biochem.* **1985**, *150*, 76.